Published in final edited form as:
Nat Med. 2011 May ; 17(5): 559–565. doi:10.1038/nm.2336.

Ablation of Fmrp in adult neural stem cells disrupts hippocampus-dependent learning

Weixiang Guo[1], **Andrea M. Allan**[1], **Ruiting Zong**[2], **Li Zhang**[1], **Eric B. Johnson**[1], **Eric G. Schaller**[1], **Adeline C. Murthy**[1], **Samantha L. Goggin**[1], **Amelia J. Eisch**[3], **Ben A. Oostra**[4], **David L. Nelson**[2], **Peng Jin**[5], and **Xinyu Zhao**[1]

[1] Department of Neurosciences, University of New Mexico School of Medicine, Albuquerque, NM 87131, USA [2] Department of Molecular and Human Genetics. Baylor College of Medicine, Houston, TX 77030, USA [3] Department of Psychiatry, University of Texas Southwestern Medical Center, Dallas, TX 75390, USA [4] Department of Clinical Genetics, Erasmus University Medical Center, Rotterdam, the Netherlands [5] Department of Human Genetics, Emory University School of Medicine, Atlanta, GA 30322, USA

Abstract

Deficiency in fragile X mental retardation protein (FMRP) results in fragile X syndrome (FXS), an inherited form of intellectual disability. Despite extensive research, how FMRP deficiency contributes to the cognitive deficits in FXS is unclear. We have previously shown that Fmrp-null mice exhibit reduced adult hippocampal neurogenesis. Since Fmrp is also enriched in mature neurons, we explored the functional significance of Fmrp expression in neural stem and progenitor cells (aNSCs) and its role in adult neurogenesis. Here we show ablation of Fmrp in aNSCs via inducible gene recombination leads to reduced hippocampal neurogenesis *in vitro* and *in vivo*, as well as significantly impaired hippocampus-dependent learning in mice. Conversely, restoration of Fmrp expression specifically in aNSCs rescues these learning deficits. These data suggest that defective adult neurogenesis may contribute to the learning impairment seen in FXS, and these learning deficits can be rectified by delayed restoration of Fmrp specifically in aNSCs.

BACKGROUND

Although the specific purpose of adult neurogenesis is not entirely clear, evidence supports its important roles in adult neuroplasticity[1–2]. Ablating aNSCs via either mouse genetics or focal irradiation leads to deficits in hippocampus-dependent learning tasks[3–8]. Conversely, treatments that can enhance neurogenesis have a positive impact on hippocampus-dependent learning[9–10]. Both adult hippocampal neurogenesis and learning are altered in several pathological conditions[1–2], but their involvement in human intellectual disability, a deficiency in learning and memory, remains elusive.

Correspondence: Xinyu Zhao (Department of Neurosciences, University of New Mexico School of Medicine, Albuquerque, NM 87131, USA; xzhao@salud.unm.edu; Starting July 1 2011: Waisman Center and Department of Neuroscience, University of Wisconsin-Madison School of Medicine and Public Health, Madison, WI 53705. xzhao@waisman.wisc.edu).

AUTHOR CONTRIBUTIONS:
W.G. and X.Z. planned the experiments, analyzed data, and wrote the manuscript. A.M.A. developed, carried out and analyzed data for behavioral analyses. W.G., L.Z., E.B.J., E.G.S., A.C.M., S.L.G. and A.M.A. carried out all the experiments. P.J. helped with mouse line acquisition and concept development. R.Z., B.A.O., and D.L.N. made *Fmr1* cON mice. A.J.E. provided *Nes-CreER*^{T2} mouse line and ROSA26-YFP mouse line and guided histological analysis.

COMPETING FINANCIAL INTERESTS:
The authors declare no competing financial interests.

Fragile X syndrome (FXS), the most common form of inherited intellectual disability, is caused by the functional loss of fragile X mental retardation protein (FMRP)[11]. Patients with FXS have an array of deficits including impaired cognition and learning, yet their overall brain morphology shows only subtle changes[12]. Although Fmrp null (*Fmr1* KO) mice perform relatively well in standard learning tests[13–15], they exhibit profound deficits in difficult association tasks[16], particularly the hippocampus-dependent trace conditioning task[17–18]. Fmrp is enriched in neurons therefore the learning deficits of FXS patients and mouse models are widely believed to result from a deficiency in the synaptic plasticity of mature neurons[19–21]. We recently reported that Fmrp regulates aNSC fate, and the loss of functional Fmrp leads to impaired adult hippocampal neurogenesis[22]. However, whether Fmrp regulation of adult neurogenesis has any functional significance in learning remains a question.

In this study, we tested the hypothesis that Fmrp plays an important role in adult neurogenesis, and therefore hippocampus-dependent learning abilities. Using inducible conditional Fmrp deletion and restoration mouse lines, we show that selective deletion of Fmrp from aNSCs leads to impaired performance on two hippocampus-dependent learning tasks. Conversely, restoration of Fmrp specifically in aNSCs rescues these learning deficits. Therefore, our data offer direct evidence in support of a critical role for adult neurogenesis in hippocampus-dependent learning and reveal that defective adult neurogenesis contributes to the learning impairment seen in FXS. Remarkably, these learning deficits can be rectified by specific restoration of Fmrp in aNSCs of adult brains, which may lead to new therapeutic interventions for FXS.

RESULTS

Deletion of Fmrp from aNSCs alters hippocampal neurogenesis

To achieve targeted deletion of Fmrp specifically in aNSCs, we generated inducible Fmrp conditional knockout mice (*Fmr1*$^{loxP/y}$*:Nes-CreER*^{T2}*:R26R-YFP* or “cKO:Cre:YFP”) by crossing Fmrp conditional knockout (*Fmr1*$^{loxP/y}$ or “Fmrp cKO”) mice[23] with inducible *Nes-CreER*^{T2} transgenic driver mice[24] and *Rosa26-stop-YFP* (*R26R-YFP*) reporter mice (Supplementary Fig. S1). Tamoxifen (Tam) injection leads to efficient Cre:LoxP recombination in Nestin$^+$ cells[25]. The male littermates, without the cKO allele (*Fmr1*$^{+/y}$*:Nes-CreER*^{T2}*:R26R-YFP* or “Cre:YFP Control”), were used as wild-type (WT) controls. At 1 day (d) post-Tam injection of adult mice, YFP$^+$ cells could be found in the DG of both cKO:Cre:YFP and Cre:YFP Control mice, and more YFP$^+$ cells could be found at 56 d post-Tam injections, indicating efficient Cre-mediated recombination (Fig. 1 and Supplementary Fig. S2). Fmrp expression was undetectable in the YFP$^+$GFAP$^+$ type 1 radial glia-like aNSCs at 1 d post-Tam (Fig. 1a) and remained absent at 56 d post-Tam (Supplementary Fig. S2a–c) in the cKO:Cre:YFP mice, compared to Cre:YFP Control mice (Fig. 1b and Supplementary Fig. S2d). Moreover, Fmrp was undetectable in both the YFP$^+$doublecortin$^+$ (YFP$^+$DCX$^+$) immature neurons (Supplementary Fig. S2e) and the YFP$^+$NeuN$^+$ mature neurons (Fig. 1c) of cKO:Cre:YFP mice, compared to Cre:YFP Control mice (Fig. 1d and Supplementary Fig. S2f). Therefore, Tam injection leads to Fmrp deletion specifically in aNSCs and in their progenies.

To determine the effects of Fmrp ablation from Nestin-expressing cells on adult DG neurogenesis, we assessed the number of YFP$^+$ cells and their phenotypes in cKO:Cre:YFP mice compared with Cre:YFP Control mice at 1, 14, 21, 28 and 56 d post-Tam (Supplementary Fig. S3a), representing critical developmental stages of new DG neurons in the adult[1]. The cKO:Cre:YFP mice had a significant lower number of YFP$^+$ cells in general, compared to Cre:YFP Control mice (Fig. 1e, f, genotype $F_{1,40} = 15.2$, $p < 0.0001$). While the number of YFP$^+$ cells in the DG of Cre:YFP Control mice showed a continuous increase

from 1 to 56 d post-Tam, the number of YFP^+ cells in cKO:Cre:YFP mice decreased initially until 14 d post-Tam before increasing (Fig. 1f, genotype x day $F_{4,40} = 6.68$, $p < 0.0001$). This reduction in the number of YFP^+ cells did not affect the overall volume of the DG (Supplementary Fig. S3b, c) and was not a result of increased apoptosis of YFP^+ cells (Supplementary Fig. S3d–f), as determined at 56 d post-Tam. Therefore, although more aNSCs were generated in the absence of Fmrp, fewer of these cells survived beyond 14 d post-Tam.

We next performed fate mapping of YFP^+ cells in the SGZ (Fig. 2a–d). We used GFAP and S100β to distinguish the type 1 radial glia-like aNSCs ($GFAP^+S100\beta^-$) from astrocytes ($GFAP^+S100\beta^+$)[26]. At 1 and 7 d post-TAM, there was no difference in the number of $GFAP^+S100\beta^-$ aNSCs between genotypes (Fig. 2e). However, starting from 14 d post-TAM, the number of $YFP^+GFAP^+S100\beta^-$ aNSCs was 21–32% higher in cKO:Cre:YFP mice compared with Cre:YFP Control mice (Fig. 2f, genotype $F_{1,40} = 5.6$, $p = 0.023$). Using Ki67 as a marker for proliferating cells, we found that the numbers of $YFP^+Ki67^+(DCX^-)$ immature cells (type 1 aNSCs + TAP cells) were higher in cKO:Cre:YFP mice compared with Cre:YFP Control mice from 14 d post-Tam and beyond (Fig. 2g, genotype $F_{1,40} = 11.99$, $p = 0.001$). Therefore, the deletion of Fmrp from Nestin-expressing aNSCs leads to increased production of aNSCs and immature cells, which is consistent with our published observation in *Fmr1* KO mice[22].

Young neurons in the DG first express DCX from 3 d post-cell cycle exit. As the neurons become mature, starting from ~2 weeks post-cell cycle exit, they lose expression of DCX but gain expression of a mature neuronal marker, NeuN[1]. Consistent with litareature[25], we observed that ~20% of DCX^+ cells was proliferating (DCX^+Ki67^+ neuroblasts), whereas the majority of DCX^+ cells were post-mitotic (DCX^+Ki67^- immature neurons). We found that the numbers of neuroblasts (Fig. 2g, $F_{1,40} = 36.1$, $p < 0.0001$), and to a less extent, post-mitotic young neurons (Fig. 2h, $F_{1,40} = 25.32$, $p < 0.0001$) were both reduced in cKO:Cre:YFP mice compared with Cre:YFP Control mice at as early as 7 d post-Tam. Therefore reduced proliferation of neuroblasts may underlie the reduced DCX^+ cells in cKO:Cre:YFP mice. Since new cells needed 3–4 weeks to reach the $NeuN^+$ mature stage, the differences between genotypes became significant at 28 d post-Tam (31% reduction), and more profound at 56 d (45% reduction) post-Tam (Fig. 2i genotype × day $F_{4,40} = 20.7$, $p < 0.0001$). Furthermore, this reduction of $NeuN^+$ neurons contrasted with the increase in the number of $S100\beta^+GFAP^+$ astrocytes at day 28 (30% increase) and day 56 (50% increase) post-Tam (Fig. 2j, genotype x day $F_{4,40} = 3.5$, $p = 0.015$). The changes in the percentage of each cell lineage among YFP^+ cells closely resembled the numbers of each cell lineage in the DG (Supplementary Fig. S4), suggesting that the altered numbers of each lineage type in cKO:Cre:YFP mice were largely due to the changes in fate specification of YFP^+ cells. Thus, selective deletion of Fmrp in $Nestin^+$ cells leads to increased proliferation, decreased neuronal differentiation and increased astrocytic differentiation *in vivo*, consistent with our previous report[22]. These phenotypic changes result from a cell-autonomous effect of Fmrp-deficiency in aNSCs.

Because Fmrp is known to regulate the maturation and synaptic plasticity of neurons[27], we analyzed the dendritic morphology of YFP^+ neurons at 56 d post-Tam (Supplementary Fig. S5a–f). The YFP^+ newborn neurons in cKO:Cre:YFP mice exhibited significant reductions in dendritic complexity as assessed by Sholl analysis ($F_{1,38} = 11.967$, $p = 0.001$), total dendritic length ($p < 0.05$), number of branching points (Nodes, $p < 0.05$), and number of dendritic ends ($p < 0.05$). Therefore, Fmrp expression in aNSCs is critical for multiple stages of neurogenesis.

Fmrp deletion alters aNSC proliferation and differentiation

To further confirm the cell-autonomous function of Fmrp in aNSCs, we isolated aNSCs from the DG of Fmrp cKO mice (*Fmr1*$^{loxP/y}$) and WT littermates (*Fmr1*$^{+/y}$). These primary DG-aNSCs possessed the same essential properties of NSCs as demonstrated previously[22]. Infection by retrovirus expressing a Cre-GFP fusion protein resulted in marked reduction of Fmrp expression in cKO cells, but not in WT cells (Supplementary Fig. S5g). While cKO cells without Cre exhibited no differences in either proliferation (Fig. 3a, b-left) or differentiation (Fig. 3c, d-left, e-left) compared with WT cells, Cre-GFP virus-infected cKO cells exhibited a 29% increase in BrdU incorporation (Fig. 3b-right, $n = 3$, $p < 0.05$), a 40% decrease in neuronal differentiation (Fig. 3d-right, $n = 3$, $p < 0.05$), and a 39% increase in astrocyte differentiation (Fig. 3e-right, $n = 3$, $p < 0.05$) compared with virus-infected WT cells. These results are consistent with our previous findings in *Fmr1* KO aNSCs[22].

Furthermore, compared with virus-infected WT aNSCs, Cre-GFP virus-infected cKO aNSCs differentiated into neurons with reduced neurite complexity as assessed by Sholl analysis (Fig. 3g, WT+Cre vs. cKO+Cre $F_{1,38} = 8.993$; $p = 0.005$), neurite length (Fig. 3h, $p < 0.05$), number of branching nodes (Fig. 3i, $p < 0.01$), and number of ends (Fig. 3j, $p < 0.05$). Therefore, Fmrp has important cell-autonomous functions at multiple stages of adult neurogenesis.

Deletion of Fmrp from aNSCs leads to impaired learning

Hippocampal neurogenesis is believed to be involved in hippocampus-dependent learning[1–2]. We hypothesized that Fmrp deletion-induced neurogenesis deficits would have a negative impact on hippocampus-dependent learning. Since *Fmr1* KO mice exhibit deficits in challenging learning tasks[16] and particularly the trace conditioning task[17–18] that require hippocampal neurogenesis[10,28], we decided to use this task to assess learning (Supplementary Fig. S6a, b). We first tested *Fmr1* KO mice and found they exhibited significantly less trace learning as shown by reduced freeze to both the training context (Fig. 4a, $F_{1,9} = 267$, $p < 0.001$) and to the tone (Fig. 4b, $F_{1,9} = 92$, $p < 0.001$) compared with WT littermates. Then we tested the cKO:Cre:YFP mice at 30 d post-Tam injection (Supplementary Fig. S6a). cKO:Cre:YFP mice exhibited significantly reduced freezing behavior in both the context test (Fig. 4c, $F_{1,12} = 55$, $p < 0.001$) and tone test (Fig. 4d, $F_{1,12} = 50$, $p < 0.001$) compared with Cre:YFP Control mice. We saw no effect of Tam on these behaviors (Supplementary Fig. S7a, b).

Since adult hippocampal neurogenesis may impact the ability of animals to discriminate between similar stimuli[3,9], we tested mice in a delayed nonmatching-to-place radial arm maze (DNMP-RAM) task designed to assess hippocampus-dependent spatial pattern separation[3] (Supplementary Fig. S6a, c). We first confirmed that Fmrp deficiency had no effect on olfaction using a buried food test (Supplementary Fig. S7c). We then tested the performance of *Fmr1* KO mice on this DNMP-RAM task. *Fmr1* KO mice performed significantly worse in both test settings, particularly in separation 2, compared with WT mice (Fig. 4e; genotype $F_{1,18} = 12.4$, $p < 0.002$). Similarly, cKO:Cre:YFP mice performed significantly worse in both separation settings compared with Cre:YFP Control littermates (Fig. 4f; genotype $F_{1,24} = 6.1$, $p < 0.0001$). On the other hand, neither *Fmr1* KO mice nor Tam-injected cKO:Cre:YFP mice exhibited deficits in tasks that do not require hippocampal neurogenesis, such as olfactory discrimination task for assessing olfactory learning and a novel object recognition task for assessing visual short-term memory (Supplementary Fig. S7d–f, S8a–b). Although anxiety has been reported in *Fmr1* KO mice under certain genetic backgrounds[17,29–30] which could potentially affect behavioral results, we observed no increased anxiety in either *Fmr1* KO or Tam-injected cKO:Cre:YFP mice (Supplementary

Fig. S8c–d). Therefore, selective deletion of Fmrp from aNSCs leads to specific deficits in highly challenging learning tasks that depend on adult hippocampal neurogenesis.

Restoration of Fmrp in aNSCs rescues learning

Next we test the hypothesis that restoration of Fmrp would rescue neurogenesis by using a Fmrp conditional restoration mouse line (*Fmr1*$^{loxP\text{-}Neo/y}$ or Fmrp cON). These mice express normal levels of Fmrp only after Cre-mediated deletion of the inserted Neo gene (Supplementary Fig. S1c). Indeed, Cre-GFP retrovirus infection could restore Fmrp expression in aNSCs isolated from Fmrp cON mice (Supplementary Fig. S5h). Without Cre-GFP virus-mediated recombination, Fmrp cON aNSCs exhibited a 30% higher proliferation rate (Fig. 5a, b-left, $p < 0.05$), 40% less neuronal differentiation (Fig. 5c, d-left, $p < 0.05$), and 40% more astrocyte differentiation (Fig. 5c, e-left, $p < 0.05$), compared with WT control aNSCs. Furthermore, these Fmrp cON aNSCs differentiated into neurons with reduced neurite complexity as assessed by Sholl analysis (Fig. 5f, g, WT vs. cON $F_{1,26} = 18.077$; $P < 0.001$), neurite length (Fig. 5h, $p < 0.05$), number of nodes (Fig. 5i, $p < 0.01$), and number of ends (Fig. 5j, $p < 0.05$). Therefore, Fmrp cON aNSCs without Cre exhibit deficits that were similar to those seen in *Fmr1* KO aNSCs[22] and Cre virus-infected Fmrp cKO aNSCs (Fig. 3). Importantly, Cre-mediated restoration of Fmrp in aNSCs rescued the proliferation, differentiation, and neurite extension deficits of cON cells (Fig. 5b-right, 5d-right, 5e-right, 5g-j), demonstrating that selective restoration of Fmrp expression in aNSCs is capable of rescuing the deficits of Fmrp-deficient aNSCs.

We then assessed whether restoration of Fmrp expression specifically in aNSCs could rescue learning deficits. We generated inducible conditional Fmrp restoration (*Fmr1*$^{loxP\text{-}Neo/y}$*:Nes-CreER*^{T2}*:R26R-YFP* or "cON:Cre:YFP") mice by crossing Fmrp cON mice with *Nes-CreER*^{T2}*:R26R-YFP* mice[24]. We designed a specific breeding strategy (Supplementary Fig. S1d) that allowed us to generate cON:Cre:YFP mice together with two essential littermate controls: *Fmr1*$^{+/Y}$*:Nes-CreER*$^{T2+/-}$*:R26R-YFP*$^{+/-}$ (Cre:YFP Control) mice that expressed functional Fmrp and *Fmr1*$^{loxP\text{-}Neo/Y}$*:R26R-YFP*$^{+/-}$ (cON:YFP Control) mice that did not express functional Fmrp, either before or after Tam injection and all mice received Tam injections. At 28 d post-Tam, Fmrp expression was restored only in Nestin^{+} aNSCs and their subsequent progenies of the cON:Cre:YFP mice (Fig. 6a, b).

We found that cON:YFP Control mice, without functional Fmrp, exhibited deficits in both context trace learning (Fig. 6c, $F_{1,10} = 93$, $p < 0.0001$) and tone trace learning (Fig. 6d, $F_{1,10} = 85$, $p < 0.0001$). On the other hand, the Tam-injected cON:Cre:YFP mice performed significantly better compared with cON:YFP Control littermates in both context trace learning (Fig. 6c, $F_{1,10} = 1665$, $p < 0.0001$) and tone trace learning (Fig. 6d, $F_{1,10} = 88$, $p < 0.0001$). Similar results were obtained for DNMP-RAM tests. The cON:YFP Control mice performed poorly in both separation 2 and separation 4 tests compared with Cre:YFP Controls (Fig. 6e. genotype $p < 0.01$), reminiscent of *Fmr1* KO mice and cKO:Cre:YFP mice (Fig. 3). However cON:Cre:YFP mice performed similarly as Cre:YFP Controls (Fig. 6e, $t(12) = 0.57$, ns). Therefore, restoration of Fmrp specifically in adult aNSCs and their progenies rescue these two hippocampus-dependent learning deficiencies.

DISCUSSION

In this study we manipulated the intrinsic properties of aNSCs in adult brains both positively and negatively without changing the surrounding niche cells or causing significant aNSC death. Our data suggest that the loss of functional FMRP in aNSCs may contribute to the cognitive deficits seen in FXS patients.

Earlier studies have found inconsistent hippocampus-dependent learning deficits in *Fmr1* KO mice[14,31–32]; however, we saw robust behavioral changes, likely for two reasons. First, we minimized variability that might affect behavioral tests by using only littermate males and by performing all tests during the dark cycle when mice were active. Second, we designed tasks that were more challenging than standard tests[16–18]. "Trace conditioning" is more sensitive for detecting hippocampal dysfunctions[17–18,33–35], than the standard "delay fear conditioning" used by others[14,31–32]. The DNMP-RAM is also a much more challenging task compared with standard radial arm maze[3].

The role of adult neurogenesis in learning and memory has long been debated. One theory is that adult DG neurogenesis is important for fine spatial distinctions[3,36–38]. Our DNMP-RAM data support this theory. Another theory proposes that adult neurogenesis is important for clearance of memories from the hippocampus and into storage in the cortex thereby maintaining the capacity of the hippocampus for establishing new memories[10,39–40]. Although not addressed directly in our current experiments, our model certainly lays the groundwork to test this theory in the future. It is possible these theories to some extent underestimate the significance of adult neurogenesis in hippocampal function, which becomes more apparent when aNSCs are altered rather than deleted. In Clelland et al[3]., ablation of neurogenesis only affected the performance of mice on difficult tasks. Our Tam-injected cKO:Cre:YFP mice with partial reduction of neurogenesis were impaired in both easy and difficult tasks. It is possible that Fmrp deficiency may have a more profound negative effect on adult neurogenesis and learning than irradiation. Synaptic competition between old and new neurons is known to occur when newborn neurons form synaptic connections with preexisting boutons in the DG[41]. Newly generated neurons have transiently enhanced synaptic plasticity[42–43]; therefore, they may have a strong transient ability to deprive preexisting synapses. New Fmrp-deficient neurons may therefore form defective synapses and interfere with existing neural networks, thereby disrupting the learning of even those easier tasks.

Therefore, Fmrp deficiency in aNSCs may impact adult hippocampus-dependent learning through several aspects, including reduced production of new DG neurons; disruption of hippocampal circuitry by introducing abnormal new DG neurons; and overproduction of astrocytes due to altered differentiation of aNSCs. Which aspect of Fmrp's regulation of adult neurogenesis contributes to the learning deficits is the next question that needs to be answered. Although altered embryonic neurogenesis in Fmrp-deficient mice and humans has been reported[44–47], the involvement of adult neurogenesis is a previously unrecognized facet in the etiology of FXS, which could point to possible new treatments for this disease. Hence, in addition to altered synaptic plasticity of mature neurons, defective neurogenesis in postnatal and adult brains could also contribute to the pathogenesis of intellectual disability in adult humans.

METHODS

Detailed methods and any associated references are available in the online version of the paper at http://www.nature.com/nm/. (Detailed Methods are provided in the "Supplementary Data and Methods"):

Animals

We performed all procedures involving live animals according to protocols approved by the University of New Mexico Animal Care and Use Committee. We generated the inducible conditional mutant and restoration mice by breeding *Nes-CreER*$^{T2+/+}$*: R26R-YFP*$^{+/+}$ homozygote male mice[24] with female *Fmr1*$^{loxP/y}$ mice[23] and female *Fmr1*$^{loxP\text{-}Neo/y}$*Nes-CreER*$^{T2+/-}$*:R26R-YF*$^{-/-}$ mice[24], respectively We genotyped the mice as previously

described [23–24,48]. Tamoxifen (Sigma-Aldrich) was performed based on a published procedure [24].

In vivo cell fate mapping

For In vivo fate mapping of YFP^+ cells, we euthanized the mice at 1, 7, 14, 28 or 56 d after the last TAM injection, by intraperitoneal injection of sodium pentobarbital and then transcardially perfused with saline followed by 4% PFA. We performed histological analysis of mouse brains as described previously with modifications[22,24,49]. For quantification of YFP^+ SGZ cells, we used 1 in 12 serial sections starting at beginning of hippocampus (relative to bregma, − 1.5 mm) to the end of hippocampus (relative to bregma, − 3.5 mm). We determined the YFP^+ cells in the granule layer and the volume (3-dimentional size) of the DG using unbiased stereology (StereoInvestigator, MBF Biosciences, Inc)[22,49]. We performed phenotypic analysis of YFP^+ cells as described[24]. We analyzed the dendritic complexity, including Sholl analysis, dendritic length, number of branches, and number of ends, using Neurolucida8 (MBF Bioscience, Inc) as described in our publication[50].

Isolation and analyses of aNSCs

We isolated aNSCs from the DG of 8 to 10-week-old male mice based on published methods[22,51]. We maintained aNSCs and carried out cell proliferation and differentiation analyses as described [22,52–53]. H van Pragg and F Gage cloned the sequence for Cre-GFP fusion protein from a published adeno associate viral vector[54] into a retroviral vector. We produced retrovirus using the method described in our previous publications[49–50,53]. For conditional deletion or restoration of *Fmr1* genes in aNSCs, we added Cre-GFP retroviruses twice (once per day) under proliferation condition for 2 d before the initiation of proliferation or differentiation assays. We routinely obtained ~100% infection efficiency. We determined the efficiency of Cre-induced recombination by using Western blotting with an anti-Fmrp antibody (1:500, Millipore). For loading controls, we were stripped and reprobed the membranes with the antibody against β-Actin (1: 1000, Sigma).

Behavioral Analyses

We performed these tests based on published methods. Trace Conditioning Tests were performed using a Coulbourn Habitest™ fear conditioning system as described[17–18,55] with modifications. DNMP-RAM test was performed using a Coulbourn Instruments radial arm maze based on published method[3]. Each day mice received 2 trials (sample + choice phase) for each of the two separations (separation 2 and separation 4) per day for 5 consecutive days. Repeated measures ANOVA between group and separations were carried out using SPSS for each experiment Post hoc Student's t-tests with Bonferroni corrections were used as needed. Object Recognition Test, Buried Food Test, and Elevated Plus Maze Test were performed based on our published papers[56–58]. Data are analyzed using ANOVA (SPSS version 18, SPSS Inc.)

Statistical Analyses

Unless specified otherwise, statistical analyses were performed using unpaired, two-tailed, Student's t-test or ANOVA. The data bars and error bars indicate mean ± standard error mean. (s.e.m). Scholl analysis was analyzed using multivariate analysis of variance (MANOVA) using SPSS statistical software.

Supplementary Material

Refer to Web version on PubMed Central for supplementary material.

Acknowledgments

We would like to thank C.T. Strauss for editing the manuscript, H. van Praag, D. Schaffer, and T. Xie for critical reading of the manuscript, members of the Zhao Lab for helpful discussions, S. J. von Hoyningen-Huene for technical assistance, D. Lagace and R. Smrt for technical help, and H. van Praag (NIH/NIA) and F.Gage (Salk Institute) for providing Cre-GFP construct. This work was supported by grants from the US NIH to XZ (MH080434 and MH078972) and DLN (HD38038 and HD024064). EGS is supported by an NIH/NIMH Career Opportunity for Research (COR) training grant (MH19101).

References

1. Deng W, Aimone JB, Gage FH. New neurons and new memories: how does adult hippocampal neurogenesis affect learning and memory? Nat Rev Neurosci. 2010; 11:339–350. nrn2822. [PubMed: 20354534]
2. Kempermann G, Krebs J, Fabel K. The contribution of failing adult hippocampal neurogenesis to psychiatric disorders. Curr Opin Psychiatry. 2008; 21:290–295. [PubMed: 18382230]
3. Clelland CD, et al. A functional role for adult hippocampal neurogenesis in spatial pattern separation. Science. 2009; 325:210–213. [PubMed: 19590004]
4. Deng W, Saxe MD, Gallina IS, Gage FH. Adult born hippocampal dentate granule cells undergoing maturation modulate learning and memory in the brain. J Neurosci. 2009; 29:13532–13542. [PubMed: 19864566]
5. Dupret D, et al. Spatial relational memory requires hippocampal adult neurogenesis. PLoS One. 2008; 3:e1959.10.1371/journal.pone.0001959 [PubMed: 18509506]
6. Farioli Vecchioli S, et al. The timing of differentiation of adult hippocampal neurons is crucial for spatial memory. PLoS Biol. 2008; 6:e246. [PubMed: 18842068]
7. Imayoshi I, et al. Roles of continuous neurogenesis in the structural and functional integrity of the adult forebrain. Nat Neurosci. 2008; 11:1153–1161. [PubMed: 18758458]
8. Saxe MD, et al. Ablation of hippocampal neurogenesis impairs contextual fear conditioning and synaptic plasticity in the dentate gyrus. Proc Natl Acad Sci U S A. 2006; 103:17501–17506. [PubMed: 17088541]
9. Creer DJ, Romberg C, Saksida LM, van Praag H, Bussey TJ. Running enhances spatial pattern separation in mice. Proc Natl Acad Sci U S A. 2010; 107:2367–2372. [PubMed: 20133882]
10. Kitamura T, et al. Adult neurogenesis modulates the hippocampus-dependent period of associative fear memory. Cell. 2009; 139:814–827. [PubMed: 19914173]
11. Penagarikano O, Mulle JG, Warren ST. The pathophysiology of fragile x syndrome. Annu Rev Genomics Hum Genet. 2007; 8:109–129. [PubMed: 17477822]
12. Lightbody AA, Reiss AL. Gene, brain, and behavior relationships in fragile X syndrome: evidence from neuroimaging studies. Dev Disabil Res Rev. 2009; 15:343–352. [PubMed: 20014368]
13. Mineur YS, Huynh LX, Crusio WE. Social behavior deficits in the Fmr1 mutant mouse. Behav Brain Res. 2006; 168:172–175. [PubMed: 16343653]
14. Dobkin C, et al. Fmr1 knockout mouse has a distinctive strain-specific learning impairment. Neuroscience. 2000; 100:423–429. [PubMed: 11008180]
15. D'Hooge R, et al. Mildly impaired water maze performance in male Fmr1 knockout mice. Neuroscience. 1997; 76:367–376. [PubMed: 9015322]
16. Brennan FX, Albeck DS, Paylor R. Fmr1 knockout mice are impaired in a leverpress escape/avoidance task. Genes Brain Behav. 2006; 5:467–471. [PubMed: 16923151]
17. Hayashi ML, et al. Inhibition of p21-activated kinase rescues symptoms of fragile X syndrome in mice. Proc Natl Acad Sci U S A. 2007; 104:11489–11494. [PubMed: 17592139]
18. Zhao MG, et al. Deficits in trace fear memory and long-term potentiation in a mouse model for fragile X syndrome. J Neurosci. 2005; 25:7385–7392. [PubMed: 16093389]
19. Krueger DD, Bear MF. Toward Fulfilling the Promise of Molecular Medicine in Fragile X Syndrome. Annu Rev Med. 201010.1146/annurev-med-061109-134644
20. Mercaldo V, Descalzi G, Zhuo M. Fragile X mental retardation protein in learning-related synaptic plasticity. Mol Cells. 2009; 28:501–507. [PubMed: 20047076]

21. Bassell GJ, Warren ST. Fragile X syndrome: loss of local mRNA regulation alters synaptic development and function. Neuron. 2008; 60:201–214. [PubMed: 18957214]
22. Luo Y, et al. Fragile x mental retardation protein regulates proliferation and differentiation of adult neural stem/progenitor cells. PLoS Genet. 2010; 6:e1000898. [PubMed: 20386739]
23. Mientjes EJ, et al. The generation of a conditional Fmr1 knock out mouse model to study Fmrp function in vivo. Neurobiol Dis. 2006; 21:549–555. [PubMed: 16257225]
24. Lagace DC, et al. Dynamic contribution of nestin-expressing stem cells to adult Neurogenesis. Journal of Neuroscience. 2007; 27:12623–12629. [PubMed: 18003841]
25. Ables JL, et al. Notch1 is required for maintenance of the reservoir of adult hippocampal stem cells. J Neurosci. 2010; 30:10484–10492. [PubMed: 20685991]
26. Raponi E, et al. S100B expression defines a state in which GFAP-expressing cells lose their neural stem cell potential and acquire a more mature developmental stage. Glia. 2007; 55:165–177. [PubMed: 17078026]
27. Jin P, Warren ST. New insights into fragile X syndrome: from molecules to neurobehaviors. Trends Biochem Sci. 2003; 28:152–158. [PubMed: 12633995]
28. Shors TJ, Townsend DA, Zhao M, Kozorovitskiy Y, Gould E. Neurogenesis may relate to some but not all types of hippocampal-dependent learning. Hippocampus. 2002; 12:578–584. [PubMed: 12440573]
29. Peier AM, et al. (Over)correction of FMR1 deficiency with YAC transgenics: behavioral and physical features. Hum Mol Genet. 2000; 9:1145–1159. [PubMed: 10767339]
30. Eadie BD, et al. Fmr1 knockout mice show reduced anxiety and alterations in neurogenesis that are specific to the ventral dentate gyrus. Neurobiol Dis. 2009; 36:361–373. [PubMed: 19666116]
31. Spencer CM, et al. Exaggerated behavioral phenotypes in Fmr1/Fxr2 double knockout mice reveal a functional genetic interaction between Fragile X-related proteins. Hum Mol Genet. 2006; 15:1984–1994. [PubMed: 16675531]
32. Van Dam D, et al. Spatial learning, contextual fear conditioning and conditioned emotional response in Fmr1 knockout mice. Behav Brain Res. 2000; 117:127–136. [PubMed: 11099766]
33. Misane I, et al. Time-dependent involvement of the dorsal hippocampus in trace fear conditioning in mice. Hippocampus. 2005; 15:418–426. [PubMed: 15669102]
34. Moore MD, et al. Trace and contextual fear conditioning is enhanced in mice lacking the alpha4 subunit of the GABA(A) receptor. Neurobiol Learn Mem. 2010; 93:383–387. [PubMed: 20018248]
35. Quinn JJ, Oommen SS, Morrison GE, Fanselow MS. Post-training excitotoxic lesions of the dorsal hippocampus attenuate forward trace, backward trace, and delay fear conditioning in a temporally specific manner. Hippocampus. 2002; 12:495–504. [PubMed: 12201634]
36. Gilbert PE, Kesner RP, Lee I. Dissociating hippocampal subregions: double dissociation between dentate gyrus and CA1. Hippocampus. 2001; 11:626–636. [PubMed: 11811656]
37. Aimone JB, Deng W, Gage FH. Adult neurogenesis: integrating theories and separating functions. Trends Cogn Sci. 2010; 14:325–337. [PubMed: 20471301]
38. Aimone JB, Wiles J, Gage FH. Potential role for adult neurogenesis in the encoding of time in new memories. Nat Neurosci. 2006; 9:723–727. [PubMed: 16732202]
39. Feng R, et al. Deficient neurogenesis in forebrain-specific presenilin-1 knockout mice is associated with reduced clearance of hippocampal memory traces. Neuron. 2001; 32:911–926. [PubMed: 11738035]
40. Stone SS, et al. Functional convergence of developmentally and adult-generated granule cells in dentate gyrus circuits supporting hippocampus-dependent memory. Hippocampus. 2010
41. Toni N, et al. Neurons born in the adult dentate gyrus form functional synapses with target cells. Nat Neurosci. 2008; 11:901–907. [PubMed: 18622400]
42. Ge S, Yang CH, Hsu KS, Ming GL, Song H. A critical period for enhanced synaptic plasticity in newly generated neurons of the adult brain. Neuron. 2007; 54:559–566. [PubMed: 17521569]
43. Schmidt-Hieber C, Jonas P, Bischofberger J. Enhanced synaptic plasticity in newly generated granule cells of the adult hippocampus. Nature. 2004; 429:184–187. [PubMed: 15107864]

44. Bhattacharyya A, et al. Normal Neurogenesis but Abnormal Gene Expression in Human Fragile X Cortical Progenitor Cells. Stem Cells Dev. 2008; 17:107–117. [PubMed: 18225979]
45. Castren M, et al. Altered differentiation of neural stem cells in fragile X syndrome. Proc Natl Acad Sci U S A. 2005; 102:17834–17839. [PubMed: 16314562]
46. Cunningham CL, et al. Premutation CGG-repeat expansion of the Fmr1 gene impairs mouse neocortical development. Hum Mol Genet. 2010
47. Pepper AS, Beerman RW, Bhogal B, Jongens TA. Argonaute2 suppresses Drosophila fragile X expression preventing neurogenesis and oogenesis defects. PLoS One. 2009; 4:e7618. [PubMed: 19888420]
48. Soriano P. Generalized lacZ expression with the ROSA26 Cre reporter strain. Nat Genet. 1999; 21:70–71. [PubMed: 9916792]
49. Smrt RD, et al. Mecp2 deficiency leads to delayed maturation and altered gene expression in hippocampal neurons. Neurobiol Dis. 2007; 27:77–89. [PubMed: 17532643]
50. Smrt RD, et al. MicroRNA miR-137 regulates neuronal maturation by targeting ubiquitin ligase mind bomb-1. Stem Cells. 2010; 28:1060–1070. [PubMed: 20506192]
51. Babu H, Cheung G, Kettenmann H, Palmer TD, Kempermann G. Enriched monolayer precursor cell cultures from micro-dissected adult mouse dentate gyrus yield functional granule cell-like neurons. PLoS ONE. 2007; 2:e388. [PubMed: 17460755]
52. Barkho BZ, et al. Endogenous matrix metalloproteinase (MMP)-3 and MMP-9 promote the differentiation and migration of adult neural progenitor cells in response to chemokines. Stem Cells. 2008; 26:3139–3149. [PubMed: 18818437]
53. Liu C, et al. Epigenetic regulation of miR-184 by MBD1 governs neural stem cell proliferation and differentiation. Cell Stem Cell. 2010; 6:433–444. [PubMed: 20452318]
54. Kaspar BK, et al. Adeno-associated virus effectively mediates conditional gene modification in the brain. Proc Natl Acad Sci U S A. 2002; 99:2320–2325. [PubMed: 11842206]
55. Paz R, Barsness B, Martenson T, Tanner D, Allan AM. Behavioral teratogenicity induced by nonforced maternal nicotine consumption. Neuropsychopharmacology. 2007; 32:693–699. [PubMed: 16554741]
56. Martinez-Finley EJ, Ali AM, Allan AM. Learning deficits in C57BL/6J mice following perinatal arsenic exposure: consequence of lower corticosterone receptor levels? Pharmacol Biochem Behav. 2009; 94:271–277. [PubMed: 19751756]
57. Harrell AV, Allan AM. Improvements in hippocampal-dependent learning and decremental attention in 5-HT(3) receptor overexpressing mice. Learn Mem. 2003; 10:410–419. [PubMed: 14557614]
58. Allan AM, et al. The loss of methyl-CpG binding protein 1 leads to autism-like behavioral deficits. Hum Mol Genet. 2008; 17:2047–2057. [PubMed: 18385101]

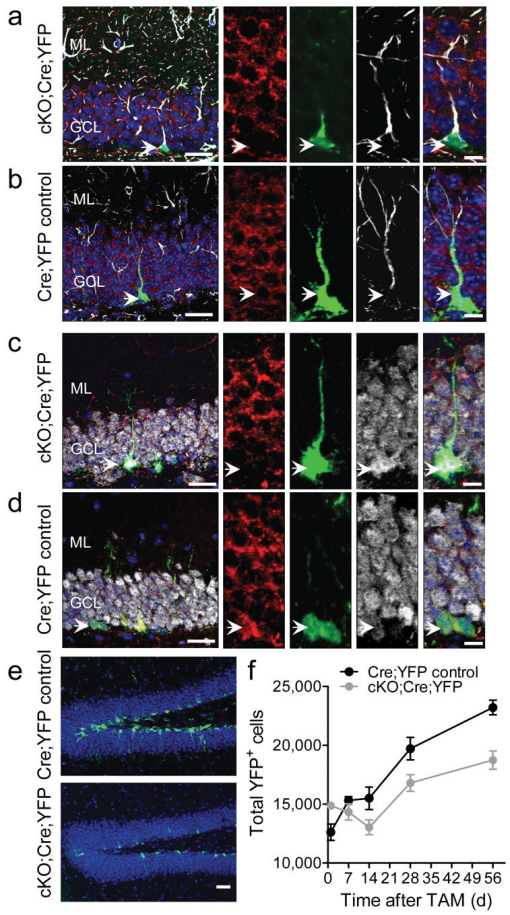

Figure 1.

Fmrp deletion in Nestin-expressing cells resulted in fewer YFP+ cells in the DG. (**a, b**) Immunohistological analyses of brain sections from cKO:Cre:YFP mice (a) and Cre:YFP Control mice (b) at 1 d post-Tam. Red, Fmrp; green, YFP; white, GFAP; blue, DAPI. Left scale bar = 20 μm; Right scale bar = 10 μm. (**c, d**) Immunohistological analyses of brain sections from cKO:Cre:YFP mice (c) and Cre:YFP Control mice (d) at 56 d post-Tam. Red, Fmrp; green, YFP; white, NeuN; blue, DAPI. Left scale bar = 20 μm; Right scale bar = 10 μm. (**e**) Sample images of YFP^+ cells in the DG at 56 d post-Tam. Green, YFP; blue, DAPI. Scale bar = 50 μm. (**f**) Quantification of the number of YFP^+ cells in cKO:Cre:YFP and Cre:YFP Control mice. ML, molecular layer; GCL, granule cell layer.

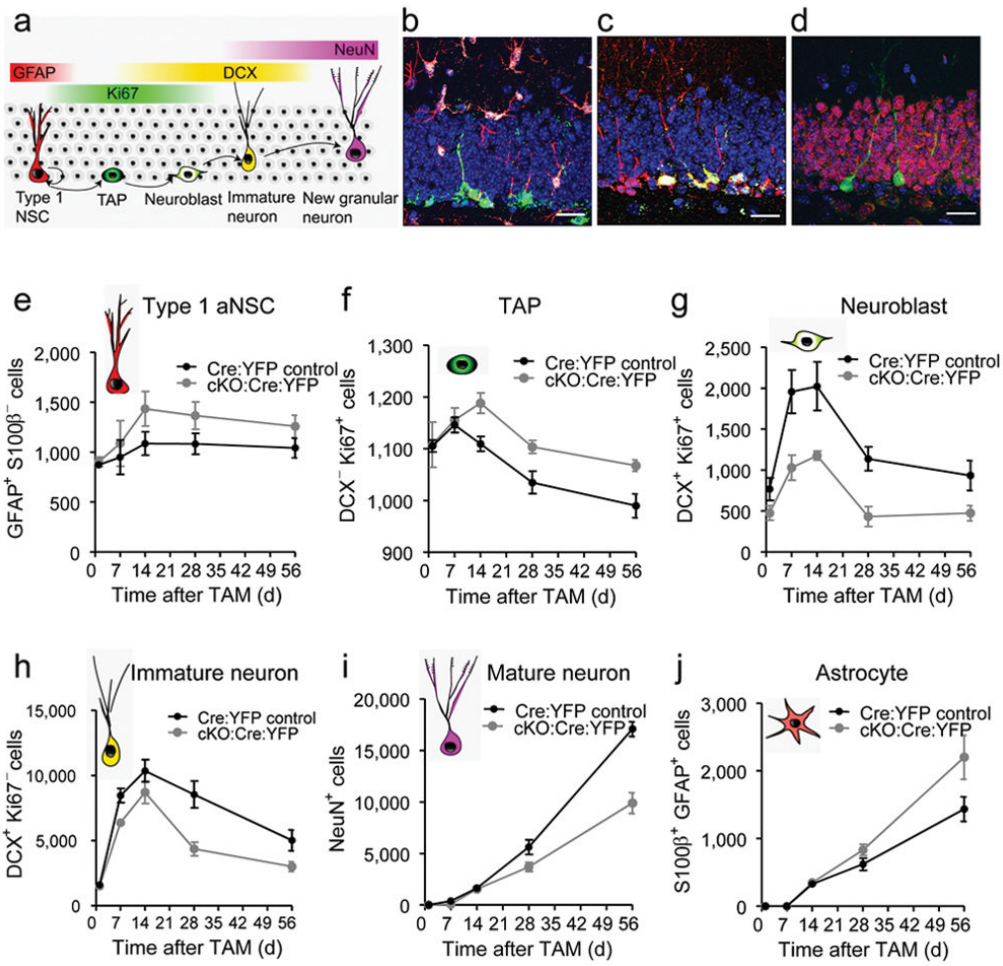

Figure 2.

Selective deletion of Fmrp in Nestin-expressing cells alters cell proliferation and fate specification of aNSCs. (**a**) Schematic diagram showing the cell lineage-specific markers across stages of neurogenesis, which were used for fate mapping. (**b–d**) Sample confocal images used for fate mapping of YFP^+ (green) cells in the DG. (b) Red, GFAP; green, YFP; white, S100β. (c) Red, DCX; green, YFP; white, Ki67. (d) Red, NeuN; green, YFP. Scale bars, 20 μm. (**e**) Quantitative comparison of the numbers of $YFP^+GFAP^+S100\beta^-$ type 1 aNSCs in the DG of cKO:Cre:YFP mice and Cre:YFP Control mice. (**f**) Quantitative comparison of the numbers of $YFP^+Ki67^+DCX^-$ transient amplifying (TAP) cells in the DG of cKO:Cre:YFP mice and Cre:YFP Control mice. (**g**) Quantitative comparison of the numbers of $YFP^+Ki67^+DCX^+$ neuroblasts in the DG of cKO:Cre:YFP mice and Cre:YFP Control mice. (**h**) Quantitative comparison of the numbers of $YFP^+Ki67^-DCX^+$ immature neurons in the DG of cKO:Cre:YFP mice and Cre:YFP Control mice. (**i**) Quantitative comparison of the numbers of YFP^+NeuN^+ mature neurons in the DG of cKO:Cre:YFP mice and Cre:YFP Control mice. (**j**) Quantitative comparison of the numbers of $YFP^+S100\beta^+$ astrocyte in the DG of cKO:Cre:YFP mice and Cre:YFP Control mice.

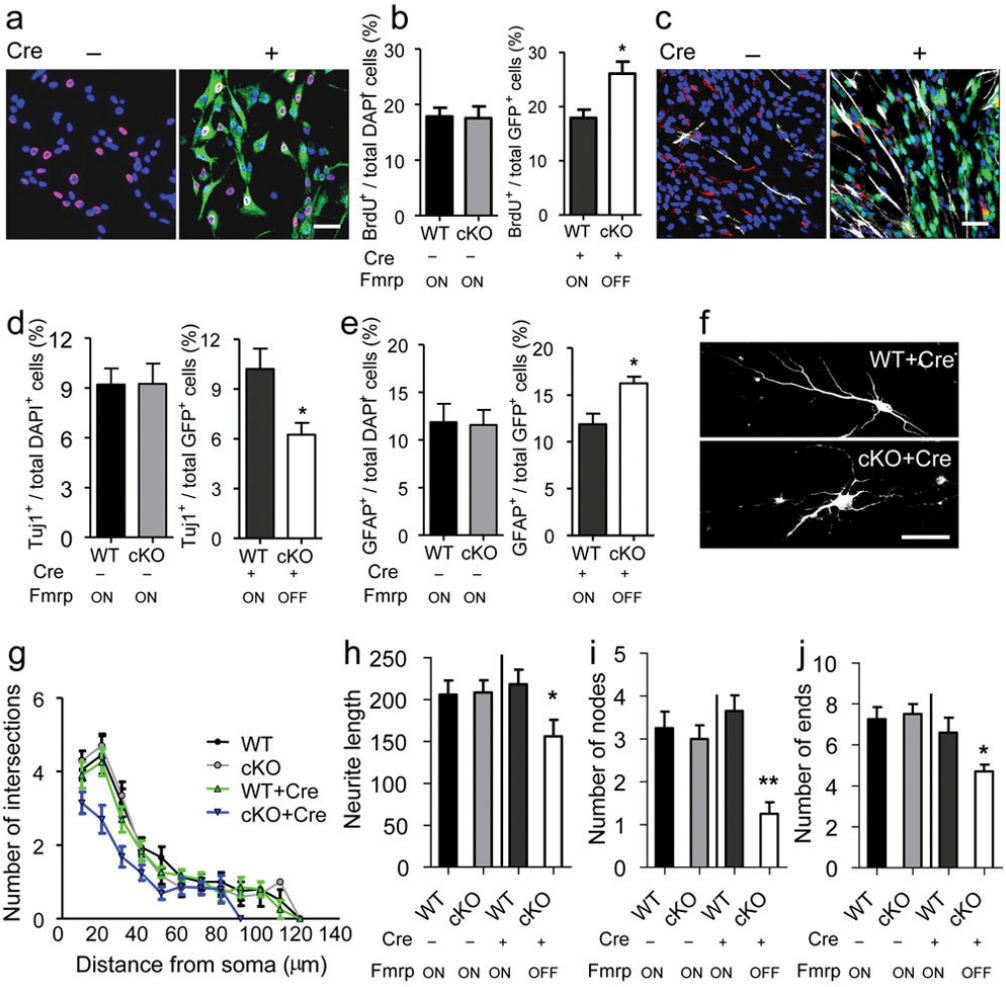

Figure 3.

Selective deletion of Fmrp in primary aNSCs isolated from adult DG results in altered proliferation and differentiation of aNSCs and reduced neurite extension of aNSC-differentiated neuron. (**a, b**) Proliferation analysis. (a) Sample image of aNSCs with (+) or without (−) Cre-GFP retrovirus infection, followed by BrdU pulse labeling and immunocytochemistry analysis. Red, BrdU; green, Cre-GFP; blue, Dapi. Scale bar, 20 μm. (b) Quantitative comparison of the percentage BrdU-labeled cells in both cKO cells and WT control cells either without (left) or with (right) Cre-GFP viral infection. (**c–e**) Differentiation analysis. (c) Sample image of differentiated aNSCs with (+) or without (−) retrovirus-Cre-GFP infection, analyzed by immunocytochemistry. Red, Tuj1; green, Cre-GFP; white, GFAP; blue, Dapi. Scale bar, 20 μm. (d, e) Quantitative comparison of the percentage $Tuj1^+$ neurons (d) and $GFAP^+$ astrocytes (e) in both cKO cells and WT control cells either without (left) or with (right) Cre-GFP viral infection. (**f**) Sample images of neurons differentiated from WT and cKO aNSCs infected with Cre-GFP-virus. Scale bar, 20 μm. (**g–j**) Neurite complexity analysis of neurons differentiated from cKO or WT aNSCs either with (+) or without (−) Cre-GFP virus-infection. (g) Scholl analysis for dendritic complexity; (h) neurite length; (i) number of dendritic nodes (branching points); (j) number of ends. *, $p < 0.05$; **, $p < 0.01$. Fmrp ON, Fmrp is expressed; Fmrp OFF, Fmrp is not expressed.

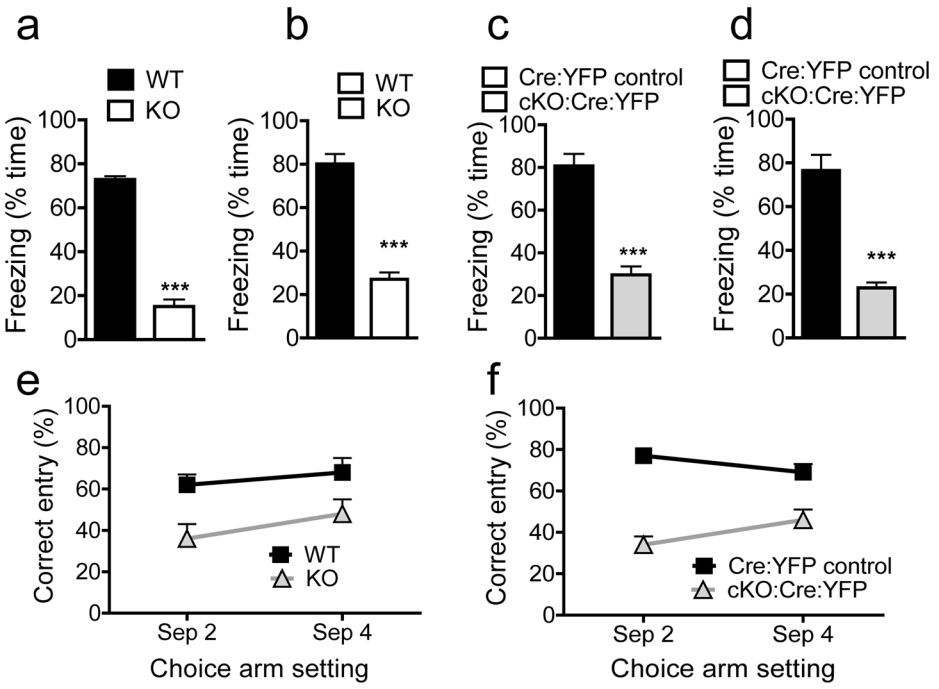

Figure 4.

Deletion of Fmrp from Nestin-positive aNSCs results in hippocampus-dependent learning deficits. (**a, b**) Context (a) and Tone (b) trace learning analyses of *Fmr1* KO mice and WT control littermates as determined by the percentage of the time that the animal spent freezing to either training context (a) or training tone (b). (**c, d**) Context (c) and Tone (d) trace learning analyses of cKO:Cre:YFP mice and Cre:YFP Control littermates as determined by the percentage time of freezing to either training context (c) or training tone (d). (**e**) DNMP-RAM analyses of *Fmr1* KO mice and WT control littermates as determined by the percentage of correct entry in both separation 2 test and separation 4 test. (**f**) DNMP-RAM analyses of cKO:Cre:YFP mice and Cre:YFP Control littermates as determined by the percentage of correct entry in both separation 2 test and separation 4 test. ***, $p < 0.001$.

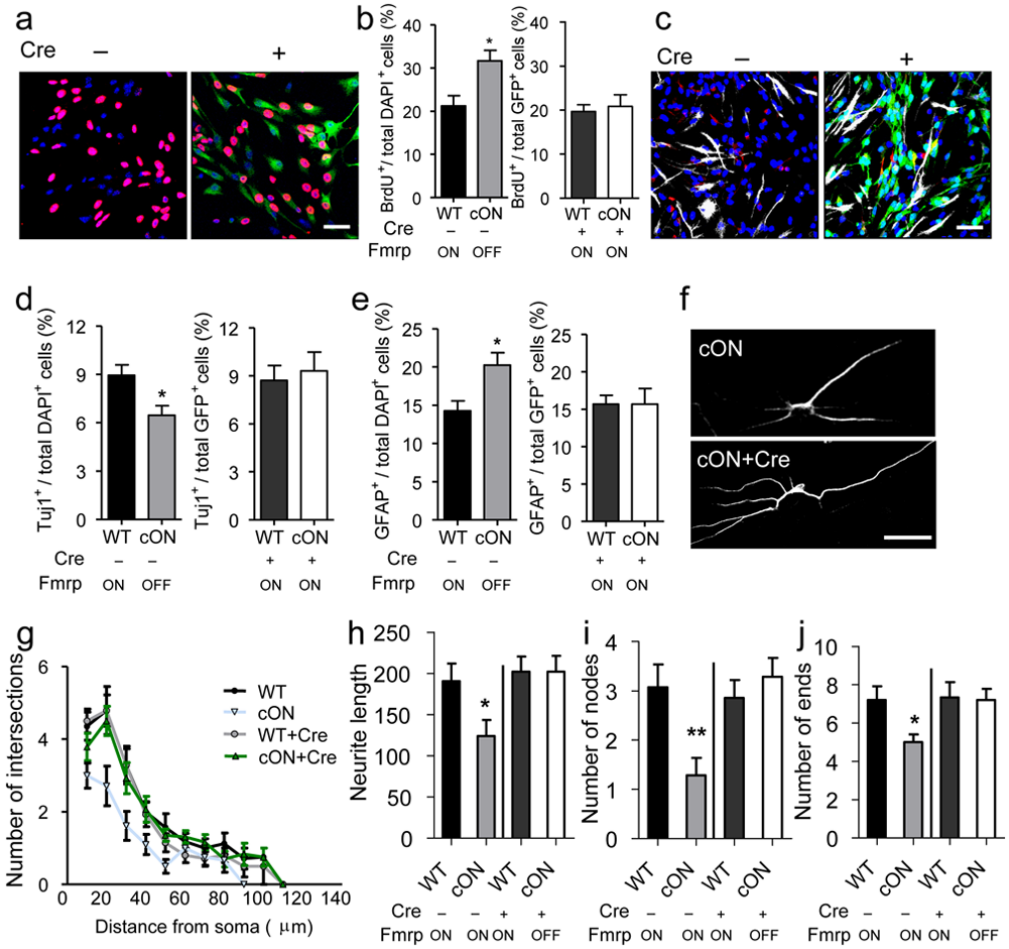

Figure 5.

Restoration of Fmrp in primary aNSCs rescues proliferation and differentiation deficits of Fmrp-deficient aNSCs and neurite extension deficits of aNSC-differentiated neurons. (**a, b**) Proliferation analysis. (a) Sample image of aNSCs with (+) or without (−) Cre-GFP retrovirus infection, followed by BrdU pulse labeling and immunocytochemistry analysis. Red, BrdU; green, Cre-GFP; blue, Dapi. Scale bar, 20 μm. (b) Quantitative comparison of the percentage BrdU-labeled cells in both cON cells and WT control cells either without (left) or with (right) Cre-GFP viral infection. (**c–e**) Differentiation analysis. (c) Sample image of differentiated aNSCs with or without retrovirus-Cre-GFP infection, analyzed by immunocytochemistry. Red, Tuj1; green, Cre-GFP; white, GFAP; blue, Dapi. Scale bar, 20 μm. (d, e) Quantitative comparison of the percentage $Tuj1^+$ neurons (d) and $GFAP^+$ astrocytes (e) in both cON cells and WT control cells either without (left) or with (right) Cre-GFP viral infection. (**f**) Sample images of neurons differentiated from WT and cON aNSCs infected with Cre-GFP-virus. Scale bar, 20 μm. (**g–j**) Neurite complexity analysis of neurons differentiated from cON or WT aNSCs with (+) or without (−) Cre-GFP virus-infection. (g) Scholl analysis for dendritic complexity; (h) neurite length; (i) number of dendritic nodes (branching points); (j) number of ends. *, $p < 0.05$; **, $p < 0.01$. Fmrp ON, Fmrp is expressed; Fmrp OFF, Fmrp is not expressed.

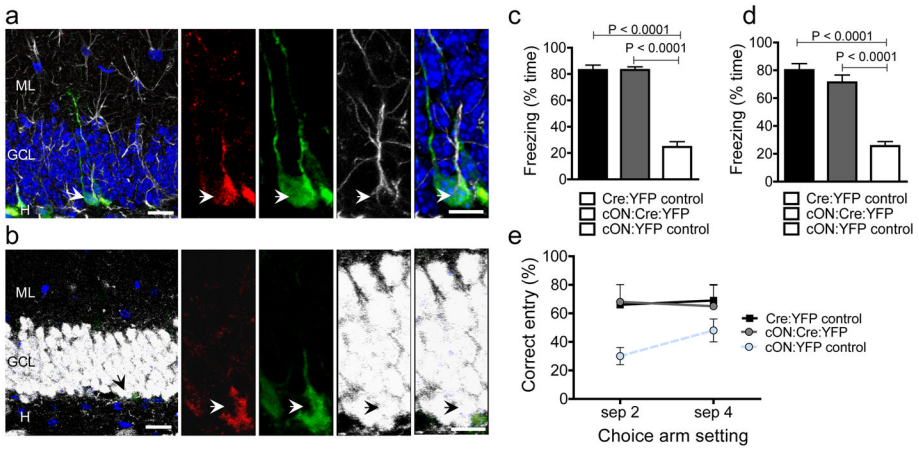

Figure 6.

Restoration of Fmrp in Nestin-expressing aNSCs and their progenies rescues hippocampus-dependent learning deficits. (**a, b**) Immunohistological analyses of brain sections from cON:Cre:YFP mice at 56 d post-Tam. (a) Red, Fmrp; green, YFP; white, GFAP; blue, DAPI. (b) Red, Fmrp; green, YFP; white, NeuN; blue, DAPI. Left scale bar = 20 μm; Right scale bar = 10 μm. (**c, d**) Context (c) and Tone (d) trace learning analyses of Cre:YFP Control mice (express Fmrp), cON:Cre:YFP mice (Fmrp restored), and cON:YFP Control (no Fmrp) littermates as determined by the percentage time of freezing to either training context (c) or training tone (d). (**e**) DNMP-RAM analyses of Cre:YFP Control (has Fmrp), cON:Cre:YFP mice (Fmrp restored), and cON:YFP Control (no Fmrp) littermates as determined by the percentage of correct entry in both separation 2 test and separation 4 test.